Heat Pipe Assisted Thermal Management of a HT PEMFC Stack

E. Firat*[,1,2], G. Bandlamudi[1], P. Beckhaus[1], A. Heinzel[1,2]
[1]Center for Fuel Cell Technology (ZBT) GmbH, Duisburg
[2]University of Duisburg-Essen
*Corresponding author: Zentrum für BrennstoffzellenTechnik (ZBT) GmbH, Carl-Benz-Straße 201, D-47057 Duisburg, Germany, e.firat@zbt-duisburg.de

Abstract: Heat management is crucial for the satisfactory operation of HT-PEM (High temperature polymer-electrolyte-membrane) fuel cells. Current work investigates the use of heat pipes in a HT PEMFC stack consisting of 24 cells, each with an active area of 300 cm². Heat pipes are known to be thermal superconductors operating on the principles of high convective heat transfer and phase transition. They can transfer large amounts of heat at high speeds in both heating and cooling applications with a higher thermal conductivity than a solid copper bar of same geometry. They are used extensively in the electronic industry. However, adapting them in fuel cell stacks in order to maintain a desired temperature level comes with challenges. The thermal load a specific heat pipe can get, the amount of heat the same can transfer and its type (groove, mesh, etc) are some of the factors to consider when choosing a suitable heat pipe. Commercially available sinter type heat pipes were selected for these investigations. COMSOL Multiphysics® based simulations were performed to analyze temperature profiles in transient mode during heating up of a 1 kW HT-PEMFC stack from room temperature to 160°C as well as cooling down from 160°C to room temperature. Calculations are performed with COMSOL Multiphysics® by using an equivalent model derived for a single heat pipe.

.

Keywords: High temperature polymer-electrolyte-membrane fuel cell (HT-PEMFC), fuel cell thermal management, heat pipe.

1. Introduction

The thermal management of HT-PEM fuel cells plays an important role in getting higher performance and stable operating conditions [1]. Heat pipes are thermal devices working based on phase transition for transmitting heat at high rates. The use of enthalpy of evaporation and condensation enables heat pipes to reach up to a 90 times higher value of effective thermal conductivity than a copper bar of the same size [2]. This makes heat pipes reasonable for HT-PEM fuel cells applications. The principle of a heat pipe and the components can be seen in Figure 1. The efficient heat removal with small temperature gradients is performed by the heat transfer from the evaporator to condenser section. The easy structure and cost-effective manufacturing are significant advantages of heat pipes [3]. The high rate of heat transfer and the wide range of operating temperature from 4[K] to 2,400[K] ensures the use in several application areas e.g. aerospace, electronics, solar systems, aeropanic, etc. [3, 4, 5, 6, 7].

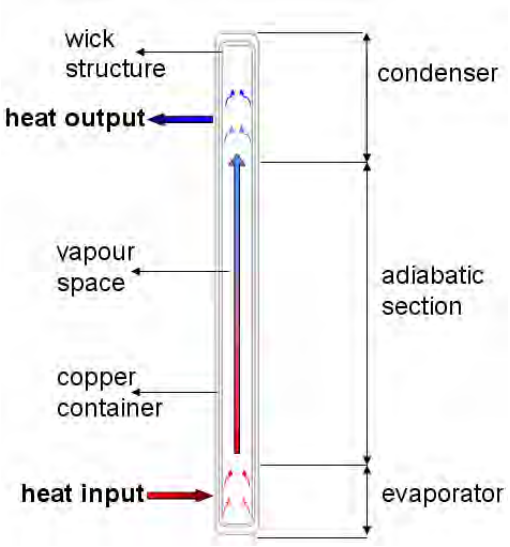

Figure 1 Principle of a heat pipe

Concerning the heat transfer limitations of heat pipes (e.g. sonic, capillary, boiling limits etc.) the sinter type of heat pipe is selected with respect to the operation temperatures [8]. Further information can be obtained from known sources [1, 2, 6, 8, 9].

2. Use of COMSOL Multiphysics®

Beside the multiphysics capabilities, COMSOL Multiphysics® has the ability to add dependent variables which facilitates the analysis of engineering problems.

2.1. Model Set-up

The simplified model of a HT-PEM fuel cell stack assembled with heat pipes can be seen in Figure 2. The thermal management of the fuel cell stack is to be analyzed and optimized with regard to heat removal and temperature distribution.

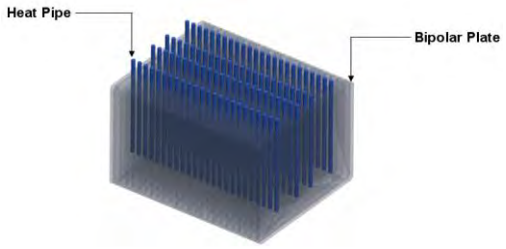

Figure 2 Simplified model of a HT-PEM fuel cell stack with 24 cells

The transient analysis of a heat pipe with phase transition is a complex phenomenon regarding the computing capabilities, inaccuracies and the size of the geometry. The 3D modelling of heat pipes with phase transition as in the examples [10, 11, 12, 13] is suitable for single heat pipe computations. For analysis of the whole fuel cell stack thermal management, the equivalent model analysis is used.

The equivalent model of a heat pipe as in [14, 15, 16] is obtained using the thermal resistance network as in Figure 3.

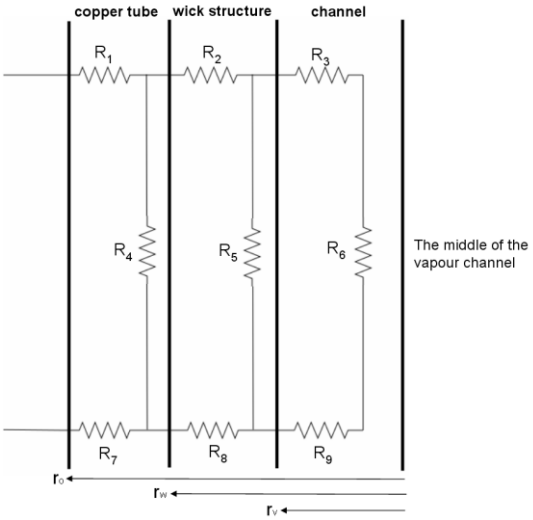

Figure 3 Thermal resistance network of a heat pipe

r_o is the outer radius of the copper tube. r_w represents radius of the wick structure and r_v is the vapour radius. The representative resistances (R1-R9) are defined as in the Table 1 with respect to the mentioned literature.

Table 1

R_i		Definition
$R_1 = \frac{\ln(r_o / r_w)}{2\pi l_e k_c}$	Eq.(1)	Evaporator tube resistance
$R_2 = \frac{\ln(r_w / r_v)}{2\pi l_e k_w}$	Eq.(2)	Evaporator wick resistance
$R_3 = \frac{\sqrt{RT_{eff}^3 / 2\pi}}{L^2 l_e r_v \rho_v}$	Eq.(3)	Liquid resistance
$R_4 = \frac{1}{k_c l}$	Eq.(4)	Tube axial resistance
$R_5 = \frac{1}{k_w l}$	Eq.(5)	Wick axial resistance
$R_6 = \frac{T_{eff} \Delta\rho_v}{LQ\rho_v}$	Eq.(6)	Vapour resistance
$R_7 = \frac{\ln(r_o / r_w)}{2\pi l_c k_c}$	Eq.(7)	Condenser tube resistance
$R_8 = \frac{\ln(r_w / r_v)}{2\pi l_c k_w}$	Eq.(8)	Condenser wick resistance
$R_9 = \frac{\sqrt{RT_{eff}^3 / 2\pi}}{L^2 l_c r_v \rho_v}$	Eq.(9)	Condenser gas-liquid interface resistance

k_i , l_i are thermal conductivity and the length of each element. ρ_v represents density. T_{eff} , Q represent effective temperature and heat transfer rate. Subscripts c and e represent condenser and evaporator sections respectively. Thermal

conductivity of the wick can be defined as in Eq.(10) [8]

$$k_w = \left\lfloor \begin{matrix} 2 + k_l / k_s - 2\varepsilon(1 - k_l / k_s) \\ 2 + k_l / k_s + \varepsilon(1 - k_l / k_s) \end{matrix} \right\rfloor \quad \text{Eq.(10)}$$

The average of the conductivity matrix Eq.(10) is used as overall thermal conductivity of wick structure. k_l, k_s are thermal conductivities of operating liquid and solid material respectively. ε (porosity) is assumed as 0.8 according to [8]. Comparing with the overall resistance, R4 and R5 can be neglected. R3, R6, and R9 are set to be zero since the heat pipes are working below limits [8, 14]. The overall resistance for the heat pipe is therefore shown in the Eq.(11).

$$R_e = R_1 + R_2 + R_7 + R_8 \quad \text{Eq.(11)}$$

The overall thermal conductivity for one heat pipe is calculated as 1,656.2[W/K.m]

2.2. Subdomain Equations

The governing equation for the heat transfer is shown in Eq.(12).

$$\rho C_p \partial T / \partial t + \nabla \cdot (-k \nabla \mathbf{T}) = Q \quad \text{Eq.(12)}$$

$\mathbf{T}$ is temperature variable and Q is the heat source. t and k represent time and thermal conductivity respectively. C_p is the specific heat capacity.

2.3. Boundary Settings

Defined boundary conditions can be seen in Figure 4.

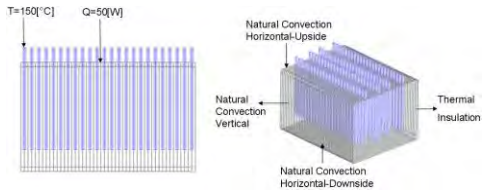

Figure 4 Boundary conditions

Overall thermal energy to be removed from the system is 50[W] for a single fuel cell. Thermal energy transferred from the fuel cell stack is defined as boundary condition. The natural heat convection on the sides of the fuel cell stack is defined using convection functions of COMSOL reference library [17]. The initial temperature is selected as 160[°C].

The element type for the geometry is selected regarding the simulation conditions. Transient analysis is performed by setting the time step as 20[sec] and time interval from 0[sec] to 1000[sec] interval.

Meshing of the fuel cell stack can be seen in Figure 5.

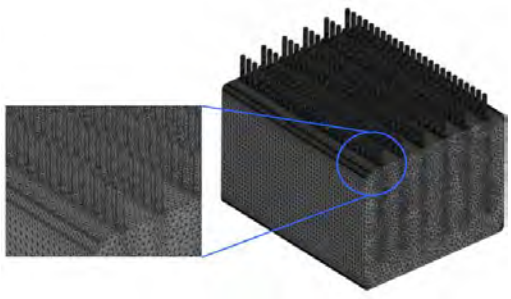

Figure 5 Meshing Elements

The model consists of 116,958 degrees of freedom. Taking the number of degrees of freedom into account, a direct solver (SPOOLES) is chosen.

3. Results

Two types of heat pipe assembly concepts are studied. Four heat pipes for each fuel cell are used in the first one. The second concept has six heat pipes assembled for each fuel cell. Heat pipes extend to the top of fuel cell stack because of the necessity to embed a thermal sink.

The transient analysis of the heat pipe assembly for selected times (200, 500, 1000[sec]) can be seen in the Figure 6, Figure 7 for both concepts respectively. The ranges for the legends are kept same for the Figure 6 and Figure 7.

Thermal distribution and the transient thermal development can be seen from the figures.

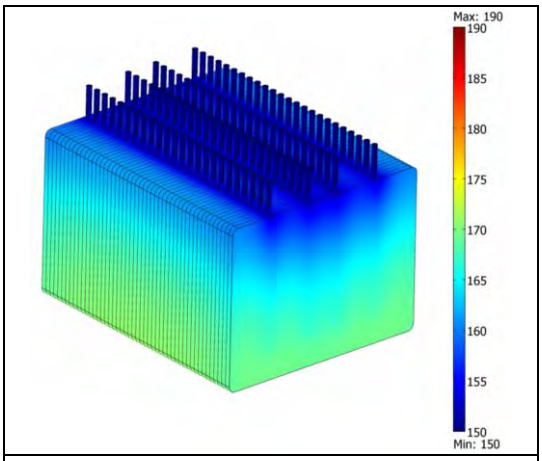

(a) $t = 200[\text{sec}]$

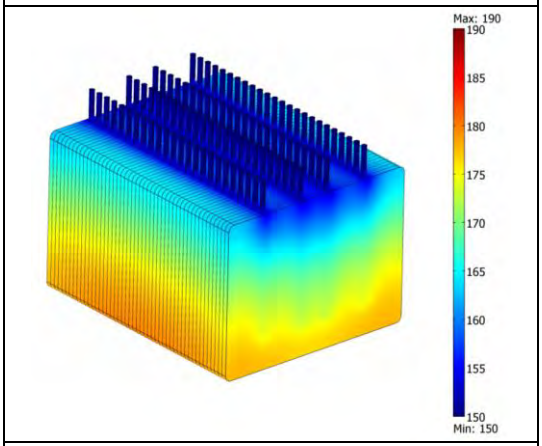

(b) $t = 500[\text{sec}]$

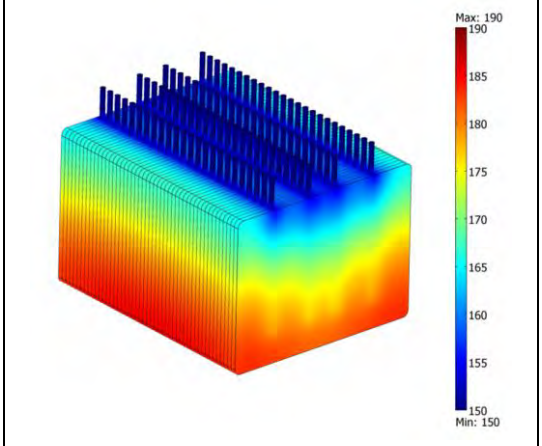

(c) $t = 1000[\text{sec}]$

Figure 6 Thermal distribution of the first concept with 4 heat pipes for each fuel cell at the time (t= 200, 500, 1000[sec])

The computations for the second concept with 6 heat pipes for each fuel cell are performed with the same boundary conditions as seen in the Figure 7.

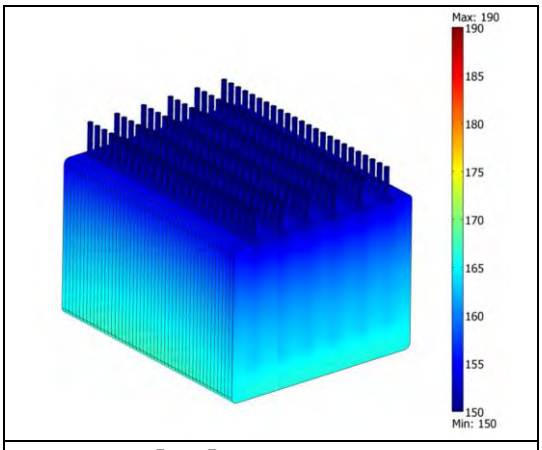

(a) $t = 200[\text{sec}]$

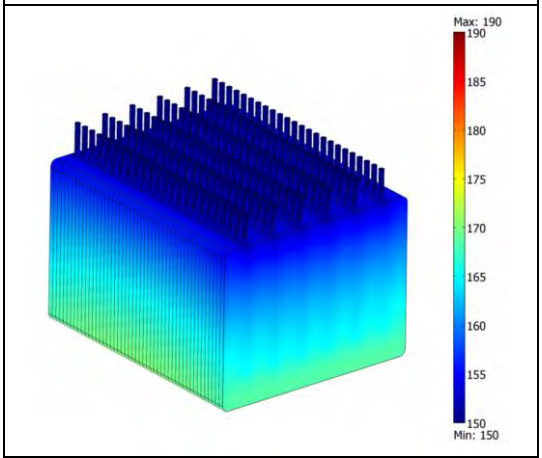

(b) $t = 500[\text{sec}]$

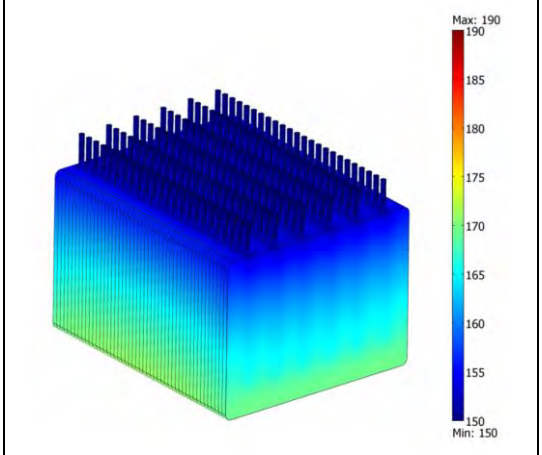

(c) $t = 1000[\text{sec}]$

Figure 7 Thermal distribution of the second concept with 6 heat pipes for each fuel cell at the time (t= 200, 500, 1000[sec])

The thermal distribution with time shows significant differences between two concepts.

The temperature peaks occurring in the middle of the fuel cell stack can be seen in Figure 6 and Figure 7. High temperature causes degradation in the fuel cell and is critical for the proper operation of fuel cell stack [17]. In order to avoid this effect, an evenly distributed temperature profile in an allowable operating temperature interval (130°C-200°C) is preferred [1]. The isothermal surfaces for both concepts are shown in Figure 8 and Figure 9 to analyze thermal gradients.

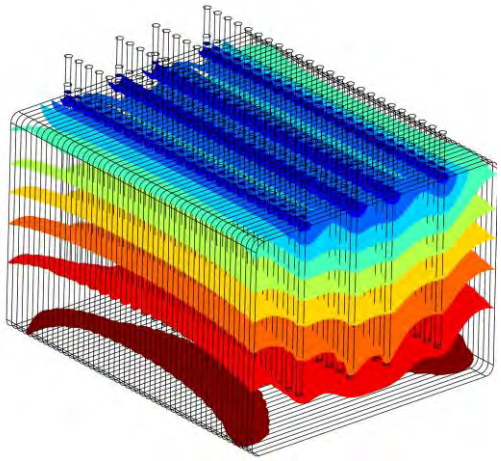

Figure 8 Isothermal surfaces for the first concept at time (t=1000[sec])

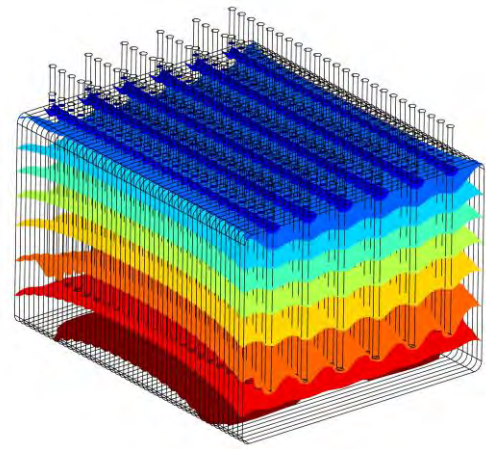

Figure 9 Isothermal surfaces for the second concept at time (t=1000[sec])

It can be seen from Figure 8 and Figure 9, that the temperature at the bottom of the stack reaches values of 180°C and temperature difference between bottom and top to 30°C. The results for the second concept with 6 heat pipes for each cell is analyzed in detail (Figure 10) by using a higher resolution of the temperature scale.

The second concept with 6 heat pipes for each cell shows better thermal distribution and lower temperature profile. The first concept can lead to exceeding the allowable temperature interval during the stack operation.

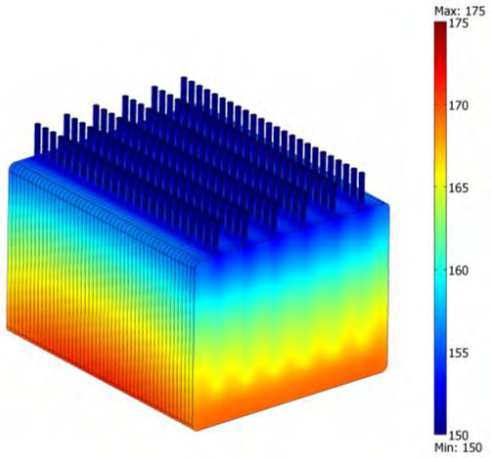

Figure 10 Thermal distribution according to the second concept with 6 heat pipes for each fuel cell at the time (t =1000[sec])

4. Conclusion

In this study, the use of heat pipes in HT-PEM fuel cell stack is investigated.

An evenly distributed temperature profile plays an important role for fuel cells. The heat removal with small temperature gradients is required. Fast heat transfer rate is necessary for dynamic operation conditions. The analysis of using heat pipes for thermal management in fuel cell stacks is performed and optimized assembly structure is investigated. The equivalent model of a single pipe is developed and integrated for 96 and 156 heat pipes in the fuel cell stack for both concepts respectively. The promising simulation results assure the application of heat pipes in HT-PEM fuel cell stacks. The simulations for the second concept with 6 heat pipes for each fuel cell show better thermal distribution and lower temperature values. Regarding the amount of heat pipes used and the ease of the montage, the first concept with four heat pipes for each fuel cell is chosen for the first experiments. The positioning and assembly structure are to be analyzed further.

5. References

1. Bandlamudi, George, Systematic Characterization of HT PEMFCs Containing PBI/H_3PO_4 Systems, Logos Verlag, (2011)

2. Faghri, A., Heat Pipe Science and Technology, Taylor & Francis, page:39-55, (1995)
3. Groll, M. Wärmerohre als Bauteile in der Energietechnik, Report
4. Srihajong, N. et al., Heat pipe as cooling mechanism in an aeroponic system, Appl. Therm.. Eng., **26**, 267-276, (2006)
5. Fiaschi, D., Manfrida, G., Model of vacuum glas heat pipe solar collectors, Proceedings of ECOS, (2012)
6. Pastukhov, V. G. et al., Miniature loop heat pipes for electronics cooling, Appl. Therm. Eng., **23**, 1125-1135, (2003)
7. Sangchandr, B., Afzulpurkar, V., A Novel Approach for Cooling Electronics Using a Combined Heat Pipe and Thermoelectric Module, J. Eng. Appl. Sci., **2 (4)**, 603-610, (2009)
8. Reay, D., Kew, P., Heat pipes page:109, Elsevier Fifth edition, (2006)
9. Peterson, G. P., An Introduction to Heat Pipes: Modeling Testing and Applications, John Wiley& Sons, (1994)
10. Zhang, Y., Faghri, A., Numerical Simulation of Condensation on a Capillary Grooved Structure, Numer Heat Transfer Part A, **39**,:227-243, (2001)
11. Li, J., Peterson, G. P., 3D Heat Transfer Analysis in a Loop Heat Pipe Evaporator with a Fully Saturated Wick, Int. J. Heat Mass Tran., **54**, 564-574 (2011)
12. Kaya, T., Goldak, J., Three-dimensional Numerical Analysis of Heat and Mass Transfer in Heat Pipes, Int. J. Heat Mass Tran., **43**, 775-785 (2007)
13. Saber, M. H., Ashtiani, H. M., Simulation and CFD Analysis of Heat Pipe Heat Exchanger Using Fluent to Increase of the Thermal Efficiency, Proceedings of 5th IASME/WSEAS International conference on Continuum Mechanics, Page:183, (2010)
14. El-Nasr, A. A., El-Haggar, S. M., Effective Thermal Conductivity of Heat Pipes, Int. J. Heat Mass Tran., **32**, 97-101, (1996)
15. Zesheng, LU., Binghui, MA., Equivalent Thermal conductivity of Heat Pipes, Front. Mech. Eng. China, **3(4)**, 462-466, (2008)
16. Korn, F, Heat Pipes and its Applications, Heat and Mass Transport, Project Report, (2008)
17. Comsol Material Library COMSOL Multiphysics® (3.5a)
18. Liu, G. et al., Studies of Performance Degradation of a High Temperature PEMFC Based on H_3PO_4-doped PBI, J. Power Sources, **162**, 547-552, (2006)